IUST
Iran University of Science and Technology

Iranian Journal of Electrical and Electronic Engineering

Journal Homepage: ijeee.iust.ac.ir

Design and Simulation of Marx Generators for Sustainable Hydrogen Production: A Focus on Stray Impedance Management

Hamid Reza Sezavar*(C.A.), Saeed Hasanzadeh*

Abstract: Marx generators that produce output pulses in the range of a few kilovolts (kV) with energies of a few millijoules (mJ) and rise times of a few nanoseconds (ns) have a variety of applications, including enhancing hydrogen production through electrolysis. In these generators, bipolar junction transistors (BJTs) operating in avalanche breakdown mode are employed as switches. This study explores the use of transistors specifically designed for avalanche breakdown to improve hydrogen generation efficiency from renewable energy sources. For this purpose, the FMMT415 transistor was implemented in the generator. The designed circuit was simulated with the transistors in avalanche breakdown mode, and the effects of various parameters on the output voltage were examined, particularly in the context of optimizing electrolysis performance. Based on the simulation results, the circuit was constructed and tested, and the differences in transistor parameters were evaluated. The simulation outcomes were then compared with the actual results. From these investigations, criteria were developed to determine the parameters that ensure suitable output voltage for Marx generator applications in hydrogen production. The optimal number of stages for the Marx generator was estimated based on the findings, highlighting its potential role in advancing sustainable hydrogen energy systems.

Keywords: Avalanche breakdown mode, Bipolar junction transistors (BJTs), Circuit simulation, Hydrogen production, Marx generator, Plasma Science, Pulse generation.

1 Introduction

GENERATION pulses with rise times in the nanosecond range has numerous applications in fields such as biological research [1], biomedical engineering [2], microwave pulse generation [3,4], non-thermal plasma processes [5], and insulation testing [6]. These pulses are also essential for characterizing material properties and are extensively used in plasma chemistry applications. Compact and efficient designs capable of producing high repetition rates and nanosecond-scale rise times are crucial for these applications. A significant use case in plasma chemistry involves laser-induced techniques for enhancing hydrogen production through electrolysis, which can improve reaction efficiency and facilitate cleaner hydrogen generation. The high-voltage pulses can initiate or sustain a plasma state in the electrolysis cell. Plasma electrolysis can significantly increase the rate of hydrogen production due to enhanced water ionization. The energy input can be optimized by applying short pulses, reducing thermal losses that occur in traditional electrolysis. Hydrogen produced through electrolysis can be generated from renewable energy sources, such as wind or solar, during peak production times. Nanosecond Marx generators could be integrated into systems that convert these intermittent power sources into hydrogen, thus acting as a buffer and enabling a stable supply.

In the chemical and petrochemical industries [7-12], there are applications that require output voltages approaching ten kilovolts (kV). In a basic Marx

Iranian Journal of Electrical & Electronic Engineering, 2025.
Paper first received 21 Jan. 2025 and accepted 10 Jun. 2025.
* The authors are with the Department of Electrical and Computer Engineering, Qom University of Technology, Iran.
E-mail: sezavar@qut.ac.ir
E-mails: hasanzadeh@qut.ac.ir
Corresponding Author: Hamid Reza Sezavar

generator utilizing bipolar junction transistors (BJTs), increasing the number of stages can enhance the output voltage. This paper investigates the impact of additional stages on transistor performance, specifically focusing on how stray impedance affects the generator's output voltage. The study includes the design and fabrication of a Marx generator employing transistors in avalanche breakdown mode, with a particular emphasis on the FMMT415 transistor type, which is commonly chosen for high-speed switching applications [13]. This transistor is preferred for its high breakdown voltage, substantial current capacity, and low stray impedance. The output voltage of the generator was simulated using a comprehensive equivalent circuit model that represents the transistors in avalanche mode [14]. Critical parameters for the transistors were identified to optimize their application in compact Marx generator configurations, and the maximum number of feasible stages for the generator was established based on the transistor characteristics.

For instance, a 500 kV Marx generator designed in [15] is intended to produce high-intensity relativistic electron beams for high-power microwave (HPM) sources. This system employs a trigger unit based on a small pulse transformer with a 30 kV output to initiate the generator. Performance was evaluated in pulse repetition frequency (PRF) mode with resistive loads and diodes, achieving a repetition rate of 80 Hz. An extensive review of Marx generators, ranging from traditional to wave installation designs, is provided in [16], covering topics such as operational methods, startup techniques, switching mechanisms, repetition rates, jitter, and various applications.

The Marx generator is fundamentally a pulse power generator designed to produce high-voltage pulses across diverse repetition rates and energy levels. This type of generator features voltage storage elements powered by a direct current (dc) supply, with the stored energy discharged to the load through fast-switching components. Effective switching is vital for shaping the output waveform and achieving very short rise times. Increasing the number of stages not only boosts the generator's output voltage but also elevates its power. Fig. 1 illustrates the schematic of a Marx generator, highlighting its operational principles, with the dc voltage source playing a pivotal role in facilitating high repetition rates during operation [17]. Marx generators are particularly adept at generating pulse voltages with varying rise times, eliminating the need for additional voltage-shaping equipment [18]. Nanosecond-scale rise times are attainable using BJTs in avalanche breakdown mode, provided that the dc voltage is appropriately configured to support a high repetition rate. Consequently, Marx generators are instrumental in pollution control applications, including pollutant particle removal [19].

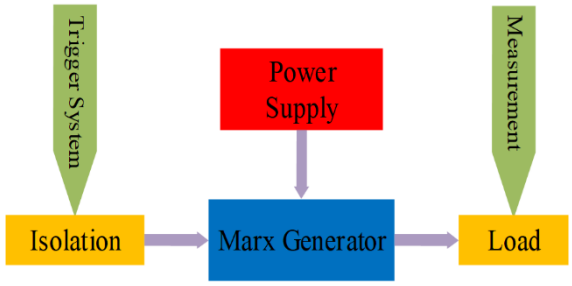

Fig 1. The design process of the Marx generator and its subsystems. The power supply is crucial in determining the repetition rate.

Various switches are employed in Marx generators, with the most significant types being spark gaps, electronic switches, and fast diodes. Electronic switches, such as metal-oxide-semiconductor field-effect transistors (MOSFETs) [20], BJTs in avalanche mode, and insulated gate bipolar transistors (IGBTs) [21], are utilized to generate pulses with short rise times and high repetition rates. The FMMT415 is a commonly used transistor for switching in avalanche breakdown mode due to its advantageous properties. Other transistors like the 2N5551 and 2N2222 possess avalanche breakdown characteristics, though they are rarely operated in avalanche mode and thus infrequently demonstrate breakdown behavior.

In high repetition rate Marx generators [19, 22], switches other than bipolar transistors are predominantly used. These generators transmit high powers, with system energies reaching several hundred joules. However, semiconductor switches with few-nanosecond rise times [7] are preferred for applications requiring lower energy and power, positioning bipolar transistors in avalanche breakdown mode as an optimal choice. Marx generators utilizing other semiconductor switches have been designed for up to a 40 kHz repetition rate [23], though their rise times and pulse durations typically exceed those of bipolar transistors. As mentioned, the output voltage of a pulsed power system increases with the number of stages, enhancing both generator power and current. Notably, in high repetition rate applications, bipolar transistors can struggle to recover from avalanche breakdown mode to off mode swiftly, which may lead to their damage. Recent research indicates that non-thermal plasma (NTP) plays a significant role in ionization, ion acceleration, ozone production, and the breaking of carbon-hydrogen (CH) bonds [24, 25]. The typical source of NTP is a Dielectric Barrier Discharge (DBD), which generates a sinusoidal output voltage [26]. However, the use of pulse power sources has recently expanded due to their advantages.

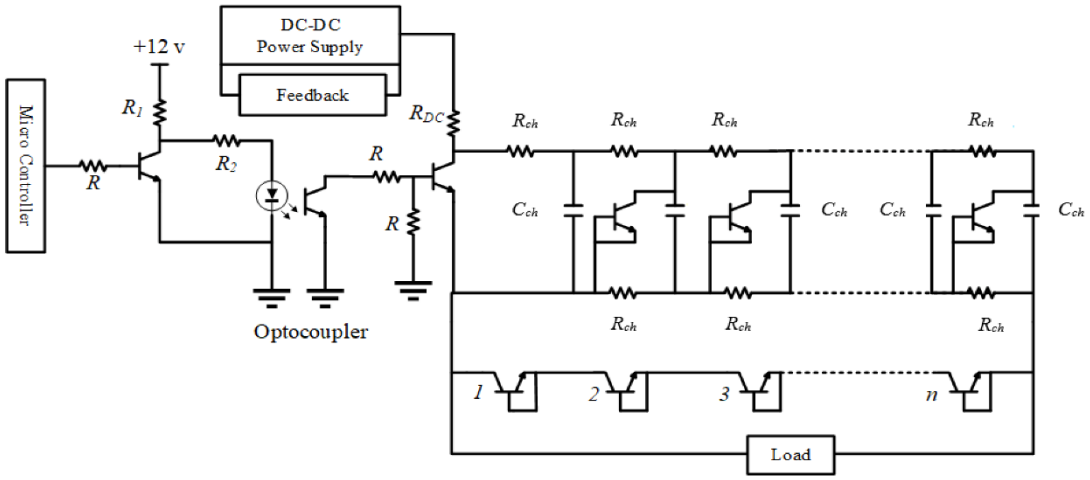

Fig 2. Complete schematic of the Marx generator with trigger system. Feedback is used to control the output voltage of the power supply. The trigger system incorporates fast transistors, and an optocoupler is utilized for insulation.

By designing a suitable BJTs-based Marx generator with low rise time and high repetition rate, NTP can be generated with significant benefits; yet, achieving the necessary power requires an increase in voltage magnitude.

Stray impedance, which includes inherent parasitic inductances and capacitances in circuit design, plays a significant role in the performance of Marx generators, mainly when applied to sustainable hydrogen production. Stray impedance impacts the output voltage stability and the rise time of the generated pulses, which are critical parameters in electrolysis processes for hydrogen generation. In the context of BJTs- based Marx generators, stray impedance can lead to voltage overshoot and ringing effects during pulse generation. When the generator rapidly switches on, stray impedance can interfere with the ideal timing and shape of the voltage pulse, resulting in a non-ideal output that may not effectively trigger the necessary electrochemical reactions in the electrolyzer. This can diminish hydrogen production efficiency and may even lead to inconsistent outputs, which is detrimental for applications relying on precise and repeated pulse inputs. Moreover, stray impedance can heavily influence the relationship between voltage magnitude and current discharge. If the impedance is not managed adequately, it can limit the effectiveness of the energy transfer from the Marx generator to the electrolyzer. As a result, a lack of knowledge or consideration of stray impedance in the design phase may compromise the generator's performance, ultimately affecting the sustainability of the hydrogen production process."

To pursue this goal, the proposed increase in stages of the Marx generator can result in the voltage magnitude of the final transistor exceeding typical limits, risking damage to the transistor. Thus, in BJTs-based Marx generators, managing the voltage magnitude is crucial for ensuring reliable operation. This paper presents simulations and experiments to analyze the behavior of transistors as switches in the Marx generator and determines critical parameters that can inform estimates of the maximum voltage magnitude or stages of the generator. This analysis demonstrates that by enhancing the characteristics of transistors, optimal voltage magnitude can be achieved, which is vital for applications in renewable energy, particularly in hydrogen production. Efficient high-voltage pulse generation is essential for improving electrolysis processes, enabling more effective hydrogen generation from renewable sources. The remainder of the paper is organized as follows: Section 2 covers Marx generator design and BJT selection; Section 3 presents simulation results and analysis; Section 4 discusses experimental verification and discussion, and finally, Section 5 provides the conclusion.

The main contributions of this paper are as follows:

- An in-depth analysis of the effects of increasing stages on BJT performance in Marx generators, focusing on stray impedance and its influence on output voltage.
- The design and simulation of a BJTs-based Marx generator that achieves high repetition rates and nanosecond rise times, validating the use of FMMT415 transistors in avalanche breakdown mode for effective pulse generation, which can enhance the efficiency of hydrogen production through electrolysis.

Experimental validation of theoretical models, identifying critical parameters that determine the

maximum voltage magnitude and optimal number of stages, along with recommendations for future designs to enhance performance in high-power applications, particularly in supporting sustainable hydrogen energy systems.

2 Marx generator design and BJT selection

The Marx generator was designed in a compact and concise form [27]. Various resistors and capacitors were installed for energy storage. When the transistors are *off*, the capacitors are connected in parallel, allowing them to store voltage via charging resistors. Fig. 2 illustrates the arrangement of the Marx generator. The primary consideration when choosing the charging path resistance is ensuring that the capacitors have a sufficiently short tim e constant, allowing them to be fully charged within the interval of two voltage pulses. The structure of the Marx generator is such that the upper stage capacitors are charged with varying time constants; for high repetition rates, they should be designed individually for each stage [1]. In this figure, R_{ch} and C_{ch} represent the resistance and capacitance charge in the Marx generator. R in the microcontroller and optocoupler is for BJT biasing. R_{dc} is resistant to the current power supply limitation. R_1 and R_2 are used for voltage division to set the optocoupler on or off. An approximate expression for the time constant of charging the n_{th} stage capacitor is as follows:

$$\tau = 5 \times n \times R_{ch} C_{ch} \tag{1}$$

This equation indicates that the capacitor at the top stage is charged later than the other capacitors, which are charged more quickly due to the calculated time constant. The Marx generator was designed with ten stages, a charging resistance of 2 kΩ, and charging capacitors of 10 nF. Consequently, the repetition rate can be increased to less than 10 kHz. It is important to note that the resistances and charging capacitance in series must exceed the resistances and load capacitances [9]. Therefore, higher resistances and charging capacitances should be employed in order to enhance the loadability of the Marx generator, even though this may reduce the repetition rate of the generator's voltage. An optimal balance must be struck between the generator load and its repetition rate, depending on the application.

The energy and power consumption for each resistance in the Marx generator can be expressed as:

$$W = \frac{n}{2} \times C_{ch} \times V^2 \tag{2}$$

$$P = (Repetition\ Rate) \times W \tag{3}$$

For a breakdown voltage of 200 V across the transistors, the energy of the generator is calculated to be 0.352 mJ. Given a repetition rate of 1 kHz, the power consumption for each charging resistor is 352 mW. The power consumption for the resistance (R_{DC}) (see Fig. 2) is approximately 3 W, necessitating the use of resistance with a high power tolerance capability. Power consumption may increase to 30 W at a repetition rate of 10 kHz, requiring high-power resistors with high impedance. The impedance can be reduced by connecting them in parallel.

The first transistor is activated by an AVR ATmega8 microcontroller, alongside a switching transistor [13]. The 2N2222 transistor is a suitable choice for switching and transferring voltage to the base of the avalanche breakdown transistor. It can be turned on and off in approximately tens of nanoseconds. A high-speed optocoupler (6N137) is employed to isolate the excitation section from the Marx generator. A pulse width modulation (PWM) signal is delivered to the 2N2222 transistor through the OCO2 pin of the microcontroller, creating the pulse voltage necessary for activating the base of the avalanche transistor. The 2N2222 transistor can also operate in avalanche breakdown mode, entering this mode at an approximate voltage of 75 V, which allows it to generate a low-jitter trigger for high repetition rates. A suitable resistive divider can be designed to create an appropriate trigger for the bipolar transistor [14]. Fig. 3 shows the components of an 10-stage Marx generator on a printed circuit board (PCB).

A boost regulator acts as a DC-to-DC step-up converter, consisting of energy storage elements, including inductors and capacitors. Fig. 4 displays a boost converter circuit. The converter operates in on and off modes. When the switch is turned on, all input energy is stored in an inductor, and when it turned off, the energy from the inductor and input energy is discharged to the output [11]. The duty cycle is the ratio of the time the switch is on to the entire period. The relationship between output and input voltages, along with the minimum required inductor and capacitor values, can be calculated using the following equations [10]:

$$V_o = \frac{V_{in}}{1 - D} \tag{4}$$

$$L_{min} = \frac{(1 - D)^2 DR}{2f} \tag{5}$$

$$C_{min} = \frac{D}{Rf\ V_r} \tag{6}$$

$$V_r = Output\ Voltage\ Ripple\ Factor \tag{7}$$

where V_o is output voltage of the boost converter. V_{in} is input voltage supplied to the boost converter. D is duty cycle, defining the proportion on the switching period during which the switch is on. L_{min} is minimum inductance required for the boost converter to operate

efficiently. R is load resistance connected to the output. F is switching frequency of the converter. $C_{min}$is minimum capacitance needed at the output to maintain voltage stability. V_r is output voltage ripple factor, indicating how much the output voltage fluctuates during operation.

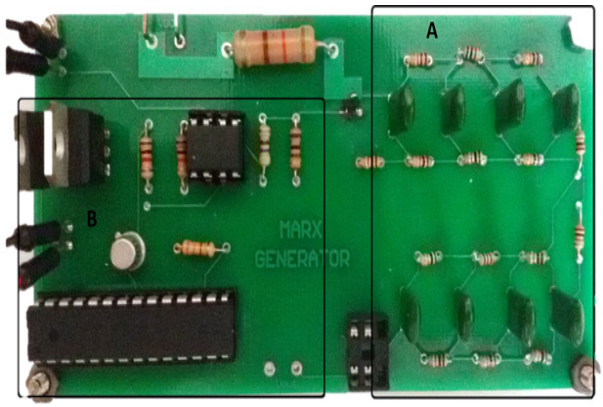

Fig 3. Ten-stage Marx generator with trigger system for the breakdown of the first transistor on a PCB. A) Marx circuit. B) Trigger circuit.

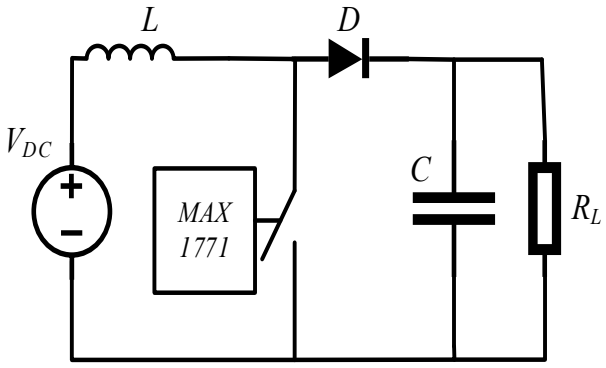

Fig 4. Circuit voltage source designed based on the boost converter. The microcontroller (MAX1771) is used to generate a trigger voltage for the switch.

It is essential that the output capacitor is sufficiently large to maintain a stable output voltage and to reduce voltage ripple. The inductor current corresponds to the circuit's input current. Input and output power can be determined by measuring the inductor current. The switching section is designed using the MAX1771 microcontroller and the IRF644 transistor. The microcontroller generates trigger pulses to control the transistor and can perform switching at frequencies up to 60 kHz. All capacitors are surface-mounted devices (SMD) with low equivalent series resistance (ESR). The ESR can be lowered further by connecting capacitors in parallel [11]. Fig. 5 shows the complete circuit of the boost converter on a PCB. It is crucial to utilize capacitors with low ESR. Ground planes are integrated throughout the circuit to enhance performance at higher frequencies. The inductor in the boost circuit is rated at 100 µH with a maximum current of 1 A. The output capacitor is 10 µF with a voltage rating of 250 V, and the ESR is about 3 Ω. The DC voltage source can generate power up to 3 W with an efficiency of 85%. The input voltage ranges from 10 to 15 V, while the output voltage ranges from 150 to 250 V.

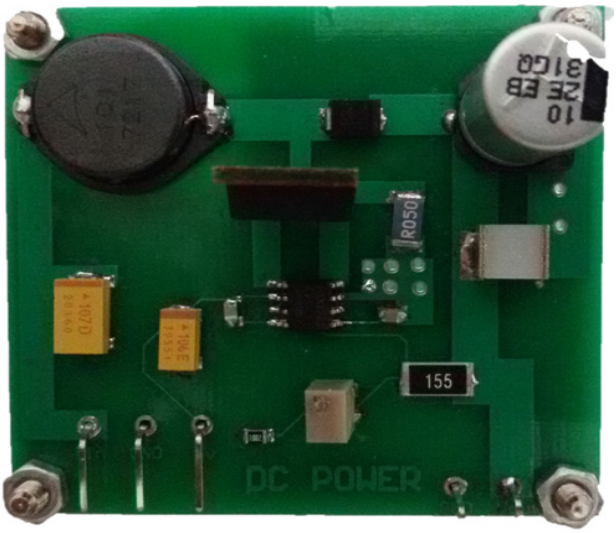

Fig 5. Complete circuit of the boost converter on a PCB. It is crucial to utilize capacitors with low ESR.

3 Simulation results and analysis

Avalanche breakdown is a phenomenon that depends on the structure of transistors, the degree of impurity, and the distribution of elements [10]. The simulation of this phenomenon requires a precise model for semiconductor devices. An avalanche breakdown model has been introduced and implemented in PSpice [7]. However, the generic model of bipolar transistors in this software, known as the Gummel-Poon model [8], is unsuitable for simulations in avalanche breakdown mode, necessitating modifications to their models. To accurately simulate avalanche breakdown in transistors, certain elements must be incorporated into the generic model of the bipolar transistor. These include voltage-controlled switches, Zener diodes for generating the breakdown voltage, specified inductors and capacitors, as well as Schottky diodes for fast switching. Zetex Company has provided a comprehensive model of avalanche breakdown for FMMT415 transistors [13]. Fig. 6 shows the equivalent circuit of a bipolar junction transistor (BJT) suitable for simulating avalanche breakdown mode. Q1 is the main transistor that is modeled using the SPICE model for transistors (Gummel-Poon). L_1, L_2, and L_3 represent the stray inductance. D_5 is the primary diode responsible for generating the breakdown voltage. In the first step, a one-stage Marx generator circuit is simulated using FMMT type transistors. The impact of different

parameters, such as energy storage capacitance, load resistance, and inductance of the path, on the output voltage was investigated. As shown in Fig. 7, a decreased capacitance value substantially reduces the peak breakdown voltage in addition to shortening the fall time. Decreasing the load resistance increases the current passing through the transistors. Consequently, high currents are generated, leading to faster breakdown of the transistors and a reduction in the rise time of the output voltage (see Fig. 8).

However, given the constant output power in the transistor, the output voltage experiences a drop. The compactness of circuits with short rise times operating in the high-frequency region is of great importance. An increased length of the circuit results in larger stray inductances. Fig. 9 illustrates the impact of increased inductance in the circuit. The rise time of the output voltage slightly increases when the stray inductance is changed from 1 nH to 100 nH. The simulated output voltage of a ten-stage Marx generator is presented in Fig. 10. The rise time of the output voltage is approximately 1 ns, with a magnitude of 2.5 kV for the Marx generator utilizing the FMMT415 transistor.

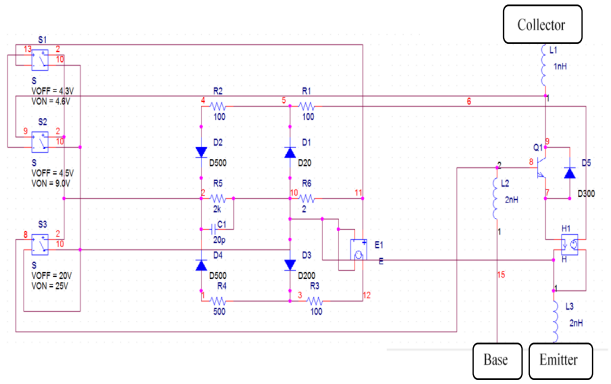

Fig 6. Equivalent circuit of a bipolar junction transistor (BJT) in avalanche breakdown mode.

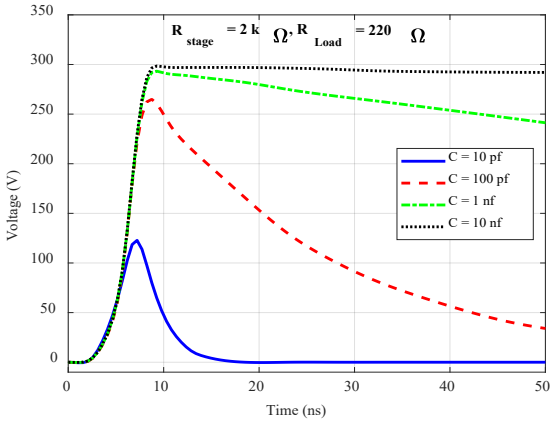

Fig 7. Influence of the energy storage stage capacitance on the output voltage of a one-stage Marx generator with FMMT415 transistor.

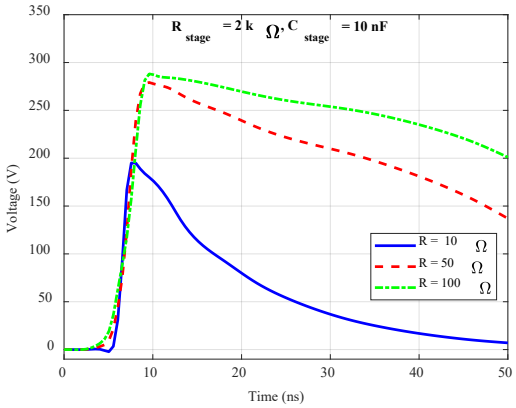

Fig 8. Influence of the load resistance on the output voltage of a one-stage Marx generator with FMMT415 transistor.

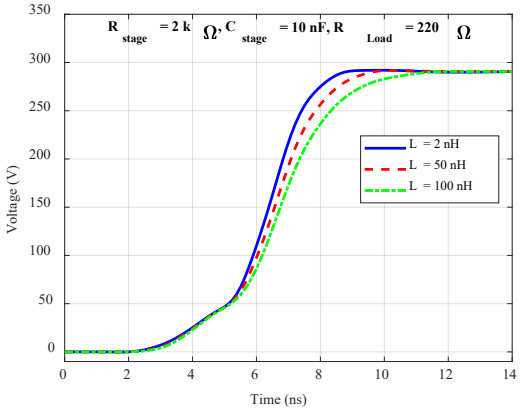

Fig 9. Influence of the circuit inductance on the output voltage of a one-stage Marx generator with FMMT415 transistor.

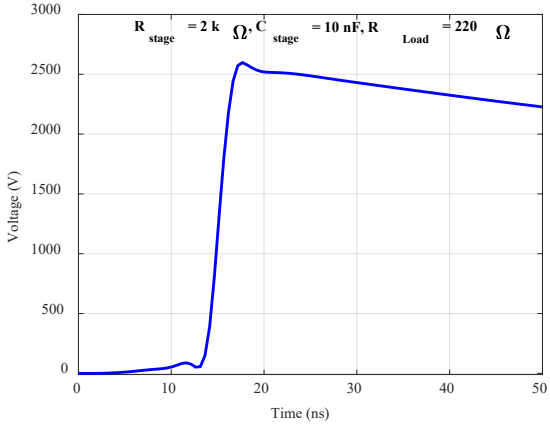

Fig 10. Simulation of output voltage of a 10-stage Marx generator with FMMT415.

According to the results shown in Fig. 9, it can be understood that the Marx generator can be designed with an increasing number of stages without significantly affecting the accurate performance of the generator. The breakdown voltage is the threshold voltage at which the dielectric material in the capacitor fails, allowing current

to flow. A lower capacitance means that less charge is stored for a given voltage. This limited charge availability during operation leads to a lower breakdown threshold as the circuit cannot sustain the necessary energy to maintain higher voltages. This highlights the critical role of capacitance in determining the operational limits of Marx generators. In fig 10, lowering the resistance enables higher current levels, affecting the transient behavior of the voltage output. The increased current causes a rapid energy transfer, resulting in a quicker output voltage rise time. However, due to Ohm's law, a corresponding drop in output voltage occurs as a portion of the available energy is dissipated across the load resistance. This trade-off between rise time and voltage underscores the importance of load characteristics in circuit design.

Figs. 11 and 12 demonstrate the results of the simulation of stray impedance based on the transistors, including the stray circuit. Fig. 11 illustrates the impact of the stray capacitance of the transistors on voltage magnitude. It is evident that by increasing the stray capacitance, the peak voltage increases due to the resonance of the stray impedance. After a few nanoseconds, the voltage stabilizes to a balanced magnitude. Stray capacitance can unintentionally act as a resonating component in the circuit due to its interaction with the present inductance. When stray capacitance increases, this can lead to resonance phenomena, whereby the energy oscillates between the inductance and capacitance. This resonance can amplify the peak voltage observed in the output, as the circuit effectively captures and reuses energy. Understanding this synergy between stray capacitance and inductance is crucial for optimizing performance in high-voltage applications.

In Fig. 12, the effect of stray inductance of the transistors is shown. With an increase in inductance, the peak voltage can be reduced, but the rise time of the voltage also decreases. Increasing the number of stages in the generators can alter the stray impedance. Consequently, by utilizing the results of the simulation of transistor parameters, it can be realized that increasing the stages of the generator to achieve the desired output voltage could lead to overvoltage conditions in the generator.

Stray inductance introduces impedance that opposes changes in current flow due to Lenz's Law. As inductance increases, the circuit becomes more "reactive," meaning it resists rapid current changes. This "damping" effect slows the voltage's rise rate, resulting in a prolonged rise time. Simultaneously, this resistance to sudden changes can decrease peak voltage, as energy is lost in overcoming this inductive reactance. The interplay between inductive and capacitive effects plays a decisive role in shaping the electrical characteristics of Marx generators.

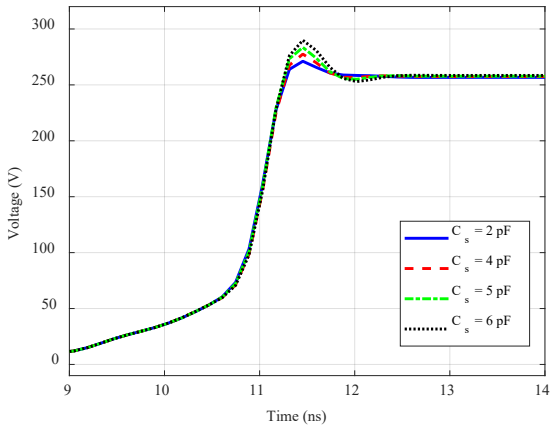

Fig 11. Effect of the stray capacitance on output voltage of a one-stage Marx generator with FMMT415 transistor.

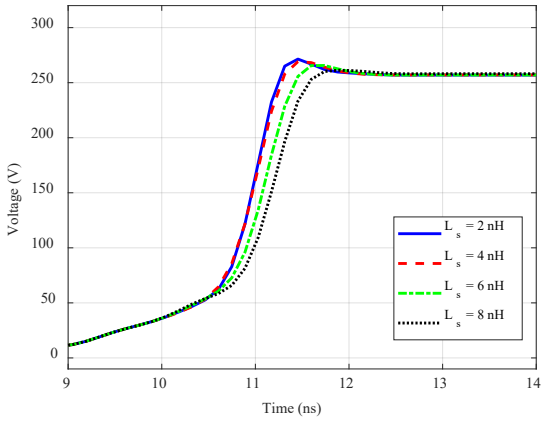

Fig 12. Effect of the stray inductance on output voltage of a one-stage Marx generator with FMMT415 transistor.

4 Experimental Verification and Discussion

Based on the design that was introduced in Sections 2 and 3, a ten-stage compact Marx generator has been constructed. The number of stages may be increased to enhance the output voltage; however, this section will explain, using the results from Figs. 11 and 12, that increasing the stages can lead to issues affecting the accurate performance of transistors. Thus, balancing the number of stages with the voltage magnitude is a critical consideration. In [28], it has been investigated that increasing the number of stages in a Marx generator influences stray impedance, mainly focusing on introducing parasitic parameters due to additional components and interconnections. As the number of stages increases, each stage contributes to the overall stray impedance through the following mechanisms:

Inductance: Each stage consists of conductive paths, which introduce stray inductance due to the components' physical layout and connection. Longer conductive paths result in greater inductance, impacting the rise time and peak voltage behavior during operation.

Capacitance: Additional stages lead to increased stray capacitance as capacitance accumulates at junctions between components and with the increased surface area of conductors. Stray capacitance can store charge and affect the transient response, potentially resulting in slower voltage rises.
Cumulative Effects: The combination of stray inductances and capacitances creates a more complex impedance profile for the circuit. Increased stages lead to intricate interactions among these elements, significantly modifying the voltage waveform and affecting peak and rise times.
Transient Response: Total stray impedance impacts the Marx generator's response to rapid switching events. The increased inductance may slow the voltage rise time, while the added capacitance could assist in managing peak voltage levels. Its intricate balance plays a critical role in the performance and reliability of the generator."

Fig. 13 demonstrates the output voltage of a ten-stage Marx generator utilizing FMMT415 transistors, which have a breakdown voltage of 230 V. The achieved output voltage is 2.5 kV (with an overvoltage of 200 V), and in this mode, the rise time is measured at 2 ns.

The increased number of stages in the designed Marx generator did not adversely affect the rise time of the output voltage, provided that the total stray inductance of the generator remained below a threshold value of a few nanohenries, as also predicted by the simulations (see Fig. 9). To achieve this objective, ground plates can be utilized, which are crucial for noise reduction as well as for minimizing the stray inductance of the circuit. Additionally, a very compact design of the generator circuit is essential; otherwise, the rise time may increase. In the case of excessively high stray inductance, fast switching is impeded, and no transistor may break down effectively. This indicates that the circuit is designed to be compact and low-jitter, and adding extra stages does not present any issues regarding the rise time performance.

A fundamental question may arise regarding the use of transistors in a Marx generator as switches in avalanche breakdown mode: How can it be ensured that the transistors perform desirably as the number of stages increases? Fig. 14 demonstrates the output voltage for different stages of the generator. In the initial stages, no overvoltage is observed, but as the number of stages increases, overvoltage and stray impedance are generated. When detecting the voltage across each transistor, important results can be observed. Fig. 15 shows the voltages of the transistors at stages 4, 6, 8, and 10 of the Marx generator. The transistors in the lower stages are operating in avalanche breakdown mode without any overvoltage; however, as the number of stages increases, the transistors in the higher stages break down at higher voltages, resulting in a decrease in their rise times. The transistors at stages 8 and 10 break down at rise times of 2 ns and 1.5 ns, respectively, with the transistor at stage 10 breaking down at approximately 350 V. Additionally, voltage stress on the transistor is clearly observable.

Based on the results of the simulations in Figs. 11 and 12, as well as the implementation results in Figs. 14 and 15, it can be understood that stray capacitance and inductance in the transistors affect the performance of the generators. Furthermore, the voltage stress caused by overvoltage can damage the last transistors in the circuit. Consequently, while increasing the number of stages in BJTs-based Marx generators is possible, it is limited, and the voltage magnitude in this type of generator is constrained by the critical parameters of the transistors.

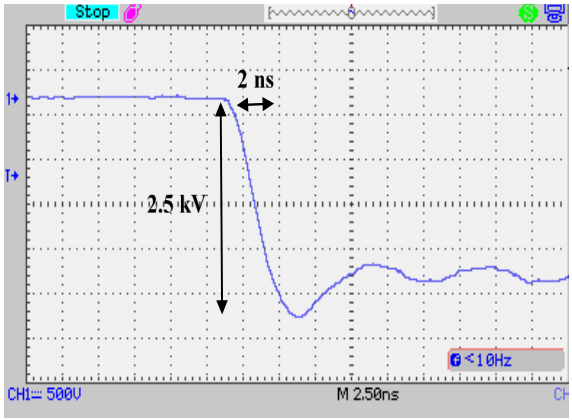

Fig 13. Output voltage of a 10-stage Marx generator utilizing FMMT415 transistors (X axis scale: 2.5 ns, Y axis scale: 500 V).

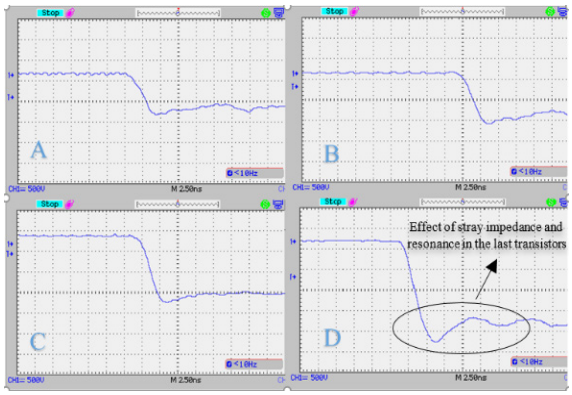

Fig 14. Output voltage at different stages of the generator (time scale: 2.5 ns). A) 4th stage. B) 5th stage. C) 6th stage. D) 10th stage (X axis scale: 2.5 ns, Y axis scale: 500 V).

Based on the simulation and experimental results, a quantitative criterion can be established for estimating the maximum number of stages in a Marx generator. Fig. 15 clearly illustrates that the transistor at stage 10 enters avalanche breakdown mode at approximately 350 V, while the breakdown voltage for the transistor in stage one is 230 V. A straightforward explanation for this is

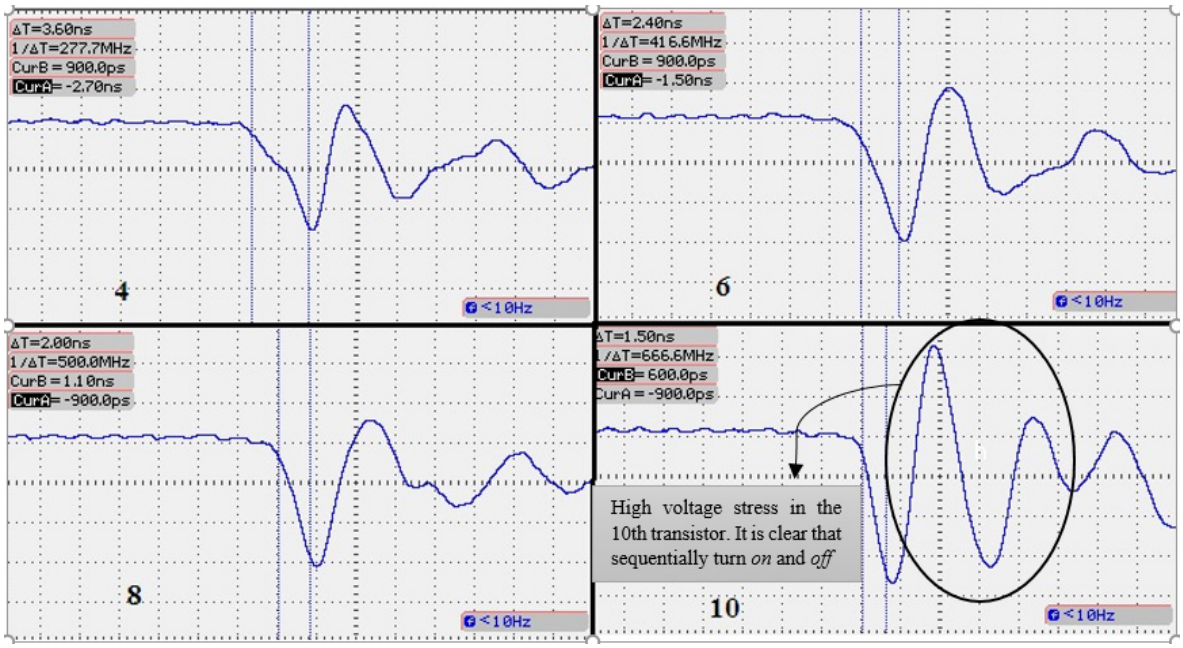

Fig 15. Output voltages of transistors at four different stages, with the stage number indicated in each figure (X axis scale: 2.5 ns, Y axis scale: 100 V).

that the overvoltage across each transistor of each stage increases by a constant factor, F_v, under ideal conditions:

$$V_n = \left(1 + F_v \times (n-1)\right) \times V_1 \quad (8)$$

where, V_1 is the voltage across the transistor of the first stage, V_n is the voltage applied to the transistor of the n-th stage, n is the number of stages, and F_v is a constant dependent on the design of the Marx generator circuit and the used type of transistor.

The maximum voltage across each stage must remain less than the maximum tolerated voltage of the transistors to ensure safe operation. Consequently, the maximum number of stages is determined based on the transistor type. For the designed compact Marx generator configuration using FMMT415 transistors, the overvoltage across ten stages is 230 V (as shown in Fig. 13). By applying equation (8) and assuming V_1=200V, the constant coefficient F_v is calculated to be approximately 0.0193. Given the maximum tolerable voltage for this type of transistor is around 320 V, the maximum number of stages that can be employed in this Marx generator design would be 21.

By analyzing the overvoltage experienced by the transistors at each stage, both before and after avalanche breakdown, the constant F_v can be further calculated. Fig. 16 presents the equivalent circuit for stage n. Initially, the transistor at stage n is off, and it is assumed that the transistor in the previous stage has turned on, transferring its breakdown voltage $V_b$through the stage capacitance to stage n. The voltage across the switch, denoted V_s, is given by:

$$V_{sw} = \left(\frac{C}{C + C_s}\right) V_b \quad (9)$$

where, C_s is the stray capacitance of the transistor, and C is the stage capacitance.

If $C \gg C_s$, then the voltage across the switch approximates V_b, causing it to turn on. Once activated, the transistor behaves like a second-order oscillatory circuit, and the maximum voltage generated across the transistor and transmitted to the next stage (V_s) can be calculated based on the parameters of this RLC circuit. At t=0 the switch is suddenly turned on. This allows current to flow through the circuit comprising Ls, Rs, and Cs. When the switch closes, the initial voltage across Ls will effectively reflect the charged state from Cs, because Cs forces the initial condition of the oscillating circuit. The inductor Ls will now react to the sudden change in voltage, and the current will start to build up. The circuit behaves as a damped RLC circuit since there are Rs, Ls, and Cs. The relevant differential equation governing the behavior of the circuit is:

$$L_s \frac{d^2 i}{dt^2} + R_s \frac{di}{dt} + \frac{1}{C_s} i = 0 \quad (10)$$

The solution to this equation describes oscillations subject to damping. The voltage Vs across the switch can be modeled as an oscillatory response influenced by the initial voltage, damping, and transient effects. The output voltage Vs can be expected to take the general form:

$$V_{sw}(t) = V_b + \Delta V(t) \quad (11)$$

The behavior can be represented as:

$$V_{sw}(t) = V_b + (\frac{t_r}{\sqrt{L_s C_s}} . e^{-\left(\frac{R_s t}{2L_s}\right)} . \sin(w_d t)) V_b \quad (12)$$

$$w_d = \sqrt{\frac{1}{L_s C_s} - (\frac{R_s}{2L_s})^2} \quad (13)$$

where w_d is the damped frequency of oscillation. Given the original equation:

$$V_s(t) = V_b + \left(\frac{t_r}{\sqrt{L_s C_s}} . e^{-\left(\frac{R_s t}{2L_s}\right)}\right) V_b \quad (14)$$

By comparing equations (8) and (14), F_v can be derived as follows:

$$F_v = \frac{t_r}{\sqrt{L_s C_s}} . e^{-\left(\frac{R_s t}{2L_s}\right)} \quad (15)$$

where, L_s and R_s represent the total series inductance and resistance of the transistor, respectively.

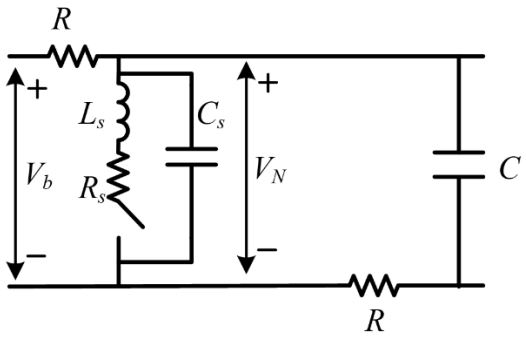

Fig 16. Equivalent circuit used for analyzing the overvoltage across the transistor.

Assuming L_s=2nH [17], R_s=6Ω [22], C_s=10pF, and t_r =2ns (rise time), the constant F_v is evaluated to be approximately 0.02 for the compact Marx generator using FMMT415 transistors, which is nearly equal to the experimental value of 0.0193.

As stage 1 enters avalanche breakdown upon triggering, stage 2 also activates. Due to the overvoltage, stage 2 will reach non-destructive avalanche breakdown more rapidly than stage 1 [17]. This cascading effect allows for sub-nanosecond rise times to be achieved. It can be concluded that a desired rise time or peak voltage can be obtained by adjusting F_v at each stage of the Marx generator. If the F_v value is high, the number of stages will decrease, and the rise time will significantly shorten. Conversely, by reducing F_v, it is possible to achieve a higher number of stages and increase the output pulse's peak voltage in a compact Marx generator.

The proposed algorithm has been designed as follows:

1. Start the design process.
2. Define the design requirements for the Marx generator.
3. Determine the desired output voltage.
4. Calculate the maximum needed number of stages for the generator.
    - Use the equation:
    $V_n = \left(1 + F_v \times (n-1)\right) \times V_1$
    - Calculate the constant F_v based on the design and component specifications.
    - Ensure that V_n is less than the maximum tolerated voltage of the transistors.
5. Determine the stray capacitance (C_s) in the circuit.
    - Consider the types of capacitors to be used.
    - Analyze the parasitic effects of the capacitors on the circuit performance.
6. Determine the stray inductance (Cs) present in the circuit.
    - Evaluate the wiring and component layout to understand inductive effects.
    - Analyze the total series inductance of the circuit components.
7. Simulate the circuit behavior using appropriate simulation tools (like SPICE).
    - Analyze the voltage and current characteristics during the simulations.
8. Optimize the design parameters based on the simulation results.
    - Adjust the number of stages, stray capacitance, and stray inductance as needed.
    - Use the equation:

$$V_s(t) = V_b + (\frac{t_r}{\sqrt{L_s C_s}} . e^{-\left(\frac{R_s t}{2L_s}\right)})$$

to estimate voltage across various stages.

9. Finalize the design specifications based on validated calculations.
10. Document the design process and resulting flowchart for future reference.
11. End the design procedure.

For validation of the proposed model, two other model has been investigated and validated with the presented model. Deng et al. (2021)[29] focused on a high-voltage nanosecond pulse generator based on an avalanche transistor Marx bank circuit coupled with a linear transformer driver (LTD). Their design targets improved efficiency and voltage capability, showcasing remarkable performances with pulse widths in the nanosecond range. Deng et al. report output voltages that reach approximately 2.4 kV, providing extensive detail about achieving high precision in pulse generation. Their architecture exhibits rise times as low as 1.8 ns, emphasizing rapid switching and minimal delay. Based on the results of Figure 17, it achieved an output voltage of 2.5 kV using a ten-stage compact Marx generator, maintaining a rise time of 2 ns. This performance is

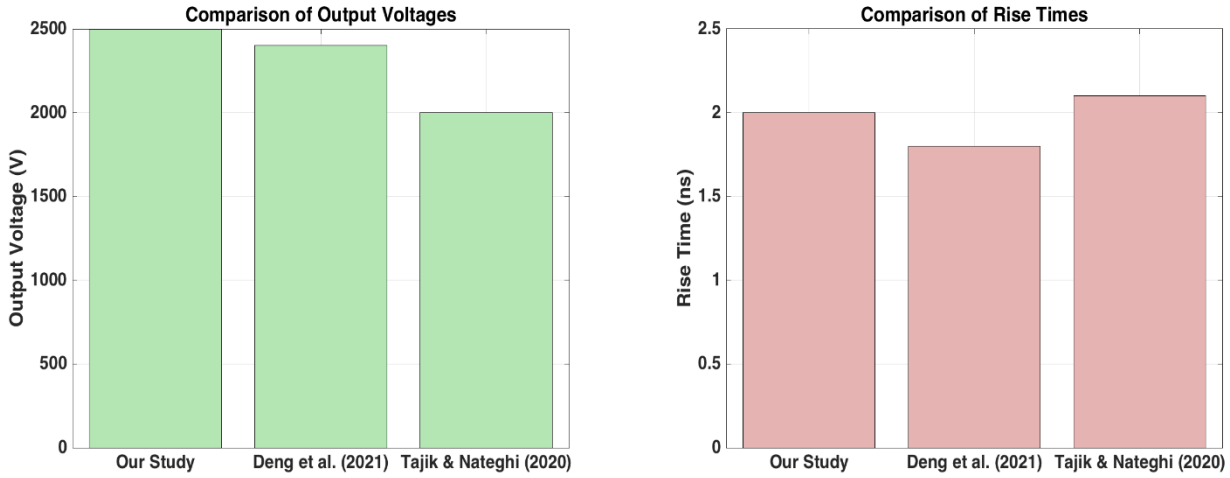

Fig 17. Validation proposed model with [29] and [30].

quite competitive and aligns closely with the findings of Deng et al., confirming the potential of avalanche transistors in achieving high-efficiency voltage applications. The close match in output voltage values illustrates that the proposed design can compete effectively with established architectures. However, the slight increase in rise time (2 ns versus 1.8 ns) could be attributed to proposed design differences in circuit layout, component selection, and stray inductance. This indicates a critical area for future optimization, especially in minimizing stray inductance, which has a pronounced effect on rise time performance.

Tajik Nateghi (2020) [30] conducted a design and simulation analysis of pulse power generators that utilize the avalanche breakdown phenomenon in bipolar junction transistors (BJTs). Their focus on performance comparison highlights the necessary design considerations for optimizing pulse characteristics. Practical output voltages in the range of 1.8 kV to 2.0 kV and pulse durations have been reported to be competitive with the nanosecond timeframe. The study emphasizes the importance of reliability in pulse generation and discusses auxiliary triggering methods to enhance performance robustness. According to Figure 17, the proposed system achieved a consistent output voltage of 2.5 kV, illustrating a distinct advantage in voltage capability compared to Tajik Nateghi's findings. The proposed design maintains a rise time of 2 ns, ensuring effective pulse generation within the desired specifications. The higher output voltage in the presented study suggests advancements in the design's efficiency and reliability, particularly through the selection of high-tolerance avalanche transistor types. Furthermore, while Tajik and Nateghi address reliability with auxiliary triggering, the proposed design's insights into minimizing stray capacitance and inductance contribute to maintaining performance consistency under operational conditions.

5 Conclusion

This paper has explored the design and performance of Marx generators based on the avalanche breakdown of bipolar junction transistors (BJTs), specifically utilizing the FMMT415 transistor type, with a focus on applications in hydrogen production from renewable energy sources. Through simulations using appropriate models for avalanche breakdown mode, it has been analyzed the impact of various parameters on generator performance, particularly as they relate to improving the efficiency of electrolysis processes for hydrogen generation. The results indicate that overvoltage caused by stray impedance can be effectively limited to achieve the desired output voltage necessary for optimizing electrolysis. A ten-stage Marx generator was designed, constructed, and tested based on the simulation findings. The study identified the maximum tolerable overvoltage of the transistors as the primary limiting factor for the number of stages in these generators. To facilitate the estimation of overvoltage experienced by the transistors, a simple model based on their stray parameters was developed. This model led to the formulation of a method for estimating the maximum number of stages achievable in the generator. The findings suggest that Marx generators utilizing FMMT415 transistors can achieve a maximum of 21 stages, offering significant potential for enhancing high-voltage pulse generation in hydrogen production applications. This research contributes to the understanding of BJT-based Marx generators and highlights the importance of managing stray parameters to optimize performance, thereby supporting the development of efficient hydrogen production technologies from renewable energy sources. The insights gained from this study lay the groundwork for future designs aimed at improving the viability and scalability of hydrogen energy systems.

Conflict of Interest

The authors declare no conflict of interest.

Author Contributions

H. R. Sezavar: Research, Software and Simulation, Original Draft Preparation, Idea & Conceptualization, **H. Hasanzadeh:** Supervision, Analysis, Revise & Editing, Verification.

Funding

No funding was received for this work.

References

[1] Yao C, Zhang X, Guo F, Dong S, Mi Y, Sun C. FPGA-controlled all-solid-state nanosecond pulse generator for biological applications. IEEE Trans Plasma Sci. 2012;40(10):2366-2372.

[2] Malik MA, Schoenbach KH, Abdel-Fattah TM, Heller R, Jiang C. Low cost compact nanosecond pulsed plasma system for environmental and biomedical applications. Plasma Chem Plasma Process. 2017;37:59-76.

[3] A. Aziznia and M. Hejazi, "Flexible Pulsed Power Generator to Create Wide Range of Pulses for Cancer Treatment," *Iranian Journal of Electrical & Electronic Engineering,* vol. 19, no. 1, 2023.

[4] M. Palati, G. Nagabhushana, and A. Sharma, "Design and development of a compact trip pulse generator," *Int. J. Electron. Electr. Eng,* vol. 4, no. 6, pp. 505-509, 2016.

[5] S. Jamali, S. N. Razavinia, and M. Bakhshzad Mahmoodi, "Investigation of the Effect of Pressure Parameter in Glow Discharge Plasma on Electron Density of Plasma," *Power, Control, and Data Processing Systems,* vol. 1, no. 1, 2024.

[6] Heeren T, Ueno T, Wang D, Namihira T, Katsuki S, Akiyama H. Novel dual Marx generator for microplasma applications. IEEE Trans Plasma Sci. 2005;33(4):1205-1209.

[7] Bai M, Leng B, Mao S, Li C. Flue gas desulfurization by dielectric barrier discharge. Plasma Chem Plasma Process. 2016;36:511-521.

[8] HafezKhiabani N, Fathi S, Shokri B. Improving plasma regeneration conditions of Pt–Sn/Al_2O_3 in naphtha catalytic reforming process using atmospheric DBD plasma system. Plasma Chem Plasma Process. 2016;36:451-469.

[9] Li S, et al. Fundamentals and environmental applications of non-thermal plasmas: multi-pollutants emission control from coal-fired flue gas. Plasma Chem Plasma Process. 2014;34:579-603.

[10] Ma T, Jiang H, Liu J, Zhong F. Decomposition of benzene using a pulse-modulated DBD plasma. Plasma Chem Plasma Process. 2016;36:1533-1543.

[11] Redolfi M, Touchard S, Duten X, Hassouni K. A simplified global model to describe the oxidation of acetylene under nanosecond pulsed discharges in a complex corona reactor. Plasma Chem Plasma Process. 2014;34:343-359.

[12] Shimizu K, Ishii T, Blajan M. Emission spectroscopy of pulsed power microplasma for atmospheric pollution control. IEEE Trans Ind Appl. 2010;46(3):1125-1131.

[13] Ogasawara A, et al. Decomposition of toluene using nanosecond-pulsed-discharge plasma assisted with catalysts. IEEE Trans Plasma Sci. 2015;43(10):3461-3469.

[14] Krishnaswamy P, Kuthi A, Vernier PT, Gundersen MA. Compact subnanosecond pulse generator using avalanche transistors for cell electroperturbation studies. IEEE Trans Dielectr Electr Insul. 2007;14(4):873-877.

[15] Shanmuganathan U, et al. A compact repetitive Marx generator for generating intense electron beams for HPM sources. IEEE Trans Electron Devices. 2023;70(3):1256-1261.

[16] Zhong Z, Rao J, Liu H, Redondo L. Review on solid-state-based Marx generators. IEEE Trans Plasma Sci. 2021;49(11):3625-3643.

[17] Li C, et al. Development and simulation of a compact picosecond pulse generator based on avalanche transistorized Marx circuit and microstrip transmission theory. IEEE Trans Plasma Sci. 2016;44(10):1907-1913.

[18] Li Z, Zhang Y, Rao J, Zhao X, Sakugawa T, Akiyama H. The switching characteristic of BJT 1 using in Marx type pulsed power generator by pspice model. In: 2015 IEEE Pulsed Power Conference (PPC); 2015:1-6.

[19] Wu Y, Liu K, Qiu J, Liu X, Xiao H. Repetitive and high voltage Marx generator using solid-state devices. IEEE Trans Dielectr Electr Insul. 2007;14(4):937-940.

[20] Li J, et al. Theoretical analysis and experimental study on an avalanche transistor-based Marx generator. IEEE Trans Plasma Sci. 2015;43(10):3399-3405.

[21] Morgan WL. The Ion Chemistry in Hydrothermal Supercritical Aqueous Sodium Chloride Fluid Ablated From a Liquid Surface. IEEE Trans Plasma Sci. 2012;40(12):3166-3173.

[22] Starikovskaia S, Anikin N, Pancheshnyi S, Zatsepin D, Starikovskii AY. Pulsed breakdown at high overvoltage: development, propagation and energy branching. Plasma Sources Sci Technol. 2001;10(2):344.

[23] Wandell RJ, Bresch S, Hsieh K, Alabugin IV, Locke BR. Formation of alcohols and carbonyl compounds from hexane and cyclohexane with water in a liquid film plasma reactor. IEEE Trans Plasma Sci. 2014;42(5):1195-1205.

[24] Rodriguez-Mendez BG, et al. Gas flow effect on E. coli and B. subtilis bacteria inactivation in water

using a pulsed dielectric barrier discharge. IEEE Trans Plasma Sci. 2012;41(1):147-154.
[25] Wang Y, Tong L, Han Q, Liu K. Repetitive high-voltage all-solid-state Marx generator for excimer DBD UV sources. IEEE Trans Plasma Sci. 2016;44(10):1933-1940.
[26] Nishida Y, Chiang HC, Chen TC, Konishi T, Cheng CZ. Hydrogen production from hydrocarbons using plasma: effect of discharge pulsewidth on decomposition. IEEE Trans Plasma Sci. 2015;43(10):3500-3506.
[27] Shimizu K, Blajan M, Kuwabara T. Removal of indoor air contaminant by atmospheric microplasma. IEEE Trans Ind Appl. 2011;47(6):2351-2358.
[28] Wen, Kaijun, Lin Liang, Ziyang Zhang, and Xiaoxue Yan. "High Power and High Repetition Frequency Nanosecond Marx Generator Based on Avalanche Transistor With Triggering Acceleration Circuit." IEEE Transactions on Power Electronics (2025).
[29] Deng, Zichen, Qi Yuan, Saikang Shen, Jiaqi Yan, Yanan Wang, and Weidong Ding. "High voltage nanosecond pulse generator based on avalanche transistor Marx bank circuit and linear transformer driver." Review of Scientific Instruments 92, no. 3 (2021).
[30] Tajik, M. R., & Nateghi, A. R. (2020, February). Design, simulation and performance comparison of pulse power generator based on the avalanche breakdown phenomenon in bipolar junction transistors. In 2020 11th Power Electronics, Drive Systems, and Technologies Conference (PEDSTC) (pp. 1-6). IEEE.

Biographies

Hamid Reza Sezavar was born in Qom, Iran, in 1991. He received a B.Sc. degree from the Sharif University of Technology, Tehran, Iran, in 2013 and a M.Sc. in electrical engineering from the University of Tehran, Tehran, Iran, in 2015. He then received his PhD in High Voltage from the University of Tehran, Tehran, Iran, in 2022. He is currently working toward an assistant professor position at Qom University of Technology. His principal research interests are High voltage engineering, outdoor insulators, Electrical discharge, and AI algorithms.

Saeed Hasanzadeh was born in Shirvan, Iran, in 1981. He earned his B.Sc. in electrical engineering from Shahroud University of Technology in 2003, followed by his MSc. and Ph.D. from the University of Tehran in 2006 and 2012, respectively. His MSc. thesis focused on High Voltage Engineering, while his Ph.D. dissertation explored Wireless Power Transfer (WPT). In 2013, he joined Qom University of Technology as an Assistant Professor in the Department of Electrical and Computer Engineering, rising to Associate Professor in 2022. He served as the department's Dean from 2018 to 2023. Dr. Hasanzadeh is an editorial board member of the Power Electronics Society of Iran (PELSI), a Technical Program Committee member of the IEEE PEDSTC Conference, and the Scientific Chair of ICREDG2025. He received Qom University of Technology's Top Research Prize in 2019 and 2023 and was recognized as an Outstanding Lecturer in 2020 and 2022. In 2023, he was named Qom province's top innovator for developing two innovative products in partial discharge detection. His research interests include power electronics, electrical machines, wireless power transfer, and high voltage engineering